COMPARISON OF GREENHOUSE GAS (GHG) EMISSIONS FROM FORWARDING RUTS IN CLEARCUTS IN ORGANIC AND MINERAL SOILS

Raitis Normunds Melniks, Zaiga Anna Zvaigzne, Arta Bardule, Martins Vanags Duka, Andis Lazdins
Latvian State Forest Research Institute "Silava", Latvia
raitis.melniks@silava.lv, zaiga.zvaigzne@silava.lv, arta.bardule@silava.lv,
martinsvanagsduka@gmail.com, andis.lazdins@silava.lv

Abstract. Soil disturbance by forwarding machinery can create ruts that alter soil structure, aeration and microtopographic water redistribution, thereby shifting post-harvest greenhouse gas (GHG) fluxes. This study assessed the short-term GHG effect of forwarding ruts in forest clearcuts on organic and moist mineral soils and developed a remote-sensing workflow to characterise rut extent for upscaling. Chamber-based measurements of CO_2, CH_4 and N_2O were carried out in 2022-2024 in six trial objects (four on organic soils and two on mineral soils), with paired sampling in ruts and adjacent undisturbed control microsites located ca. 4-5 m from ruts; organic-soil sites were harvested in winter 2022 and the monitoring design ensured multi-season post-harvest time series (including pre-harvest data availability for part of the organic-soil sites). Across organic-soil clearcuts, the combined $CO_2 + CH_4 + N_2O$ flux expressed as CO_2 equivalents was higher in ruts (537.1 ± 130.1 mg CO_2-eq$\cdot m^{-2} \cdot h^{-1}$) than in controls ($402.2 \pm 33.1$ mg CO_2-eq$\cdot m^{-2} \cdot h^{-1}$), i.e. a 33.5% increase, with the response attributed to rut-induced wetter and more anaerobic conditions that enhance CH_4 production while constraining aerobic CO_2 formation. In moist mineral soils, the rut–control increase in total GHG flux was smaller (16.7%), indicating pronounced soil-type dependence. For operational monitoring, a LiDAR–DEM approach with automated rut detection and classification (including cross-profile based depth/width characterisation) was applied at regional scale; in 38 clearcut stands on peatland forest types, ruts were observed in 24 stands (≥ 30 m of ruts deeper than 20 cm), and automated mapping underestimated rut length by ~37% relative to manual interpretation, highlighting the need for calibration and auxiliary constraints (e.g., machine GPS tracks) when scaling rut-related GHG impacts.

Keywords: ruts, greenhouse gas, mineral soil, organic soil, forest; harvesting.

Introduction

Forwarding on strip-roads is an essential element of cut-to-length harvesting, yet repeated machine passes can induce soil compaction and form ruts that persist as microtopographic depressions with altered pore structure and hydraulic connectivity. Across forest soil types, compaction reduces macroporosity and gas diffusivity while increasing water-filled pore space, thereby shifting the balance between aerobic and anaerobic microbial processes and modifying CO_2, CH_4 and N_2O fluxes. Mechanistically, reduced oxygen availability and higher moisture can suppress aerobic respiration while promoting methanogenesis and, depending on nitrogen availability and redox dynamics, can either stimulate or constrain N_2O production pathways (e.g., coupled nitrification – denitrification and denitrifier reduction of N_2O). Evidence from forest soils shows that compaction can decrease CH_4 consumption and change N_2O emissions, demonstrating that the direction and magnitude of responses are context dependent and mediated by physical constraints on diffusion and substrate supply [1].

Reducing greenhouse gas emissions from forest soils is important for climate change mitigation, particularly in wet and organic soils where small changes in aeration and water regime can substantially alter CO_2, CH_4 and N_2O fluxes. Several mitigation directions have been proposed in forestry and peatland management, including the avoidance of soil disturbance during harvesting, the use of low-impact or seasonal harvesting technologies, hydrological restoration or rewetting, and the substitution of fossil energy with forest biomass. However, these measures may involve trade-offs. For example, wetter conditions and reduced aeration may suppress aerobic CO_2 production but can also promote CH_4 formation, while biomass extraction or residue removal may contribute to fossil-fuel substitution but must be balanced against soil fertility and biodiversity considerations. Therefore, mitigation-oriented forest management requires site-specific evidence on how particular disturbances, such as forwarding ruts, modify the balance among the major greenhouse gases.

Rut formation is not random: it is strongly conditioned by soil moisture, soil texture/structure, traffic intensity and operational choices. In boreal fine-grained soils, rut depth has been shown to increase with high soil moisture and cumulative load effects, highlighting the role of hydrometeorological windows and traffic planning in risk management [2]. Landscape-scale assessments further demonstrate that rutting probability integrates soil type and wetness proxies (e.g., depth-to-water) alongside traffic

intensity and infrastructure constraints [3]. Because ruts can create localised “hotspots” of anaerobic conditions even within otherwise aerated stands, their biogeochemical influence may be spatially concentrated but disproportionately important when aggregated over operationally damaged area.

A key unresolved question is how rut-driven GHG responses differ between organic soils and wet mineral soils after clear-felling. Organic soils (peaty substrates) typically contain large carbon stocks, high water retention capacity and a propensity for anaerobiosis; thus, rutting may rapidly enhance CH_4 formation while modifying CO_2 production via oxygen limitation and altered decomposition kinetics. In contrast, moist mineral soils often exhibit lower total carbon stocks but can develop perched water and gleyic features that intermittently constrain oxygen diffusion, suggesting that rut impacts may be episodic and tightly coupled to rainfall-driven saturation and traffic-induced compaction. The limited availability of paired rut–control flux datasets across these soil types has constrained the development of robust emission factors and has left national-scale accounting largely reliant on generic assumptions rather than disturbance-explicit activity data [4; 5].

Within this context, the present study quantifies short-term post-harvest GHG flux differences between forwarding ruts and adjacent undisturbed microsites in clearcuts on organic soils and on moist mineral soils, focusing on CO_2, CH_4 and N_2O. The study explicitly frames ruts as a microtopographic and physical disturbance that modifies aeration and hydrology and therefore the process-level controls on gas exchange. The scope includes a comparative component between soil groups and a methodological component aimed at supporting operational upscaling through rut detection and extent characterisation. As preliminary evidence for wet mineral soils, the pilot study conducted in two spruce clearcuts on Podzolic Gley soils showed substantially higher CH_4 emissions in ruts than in controls during summer – autumn monitoring, whereas CO_2 differences were minor and N_2O tended to be higher in controls, consistent with aeration-driven differences in methane production/oxidation and nitrogen turnover [6].

By integrating paired flux measurements with a cross-soil comparison, this work addresses two practical knowledge gaps that currently limit mitigation-oriented forest operations and GHG reporting: first, the degree to which rut-induced GHG responses are soil-type specific (organic versus moist mineral soils) under comparable post-clearcut conditions; and second, the feasibility of translating plot-scale flux contrasts into stand-scale impacts through spatially explicit information on rut occurrence and severity. This focus allows the study to address a practical mitigation question: whether reducing rut formation in clearcuts, especially on organic soils, may lower short-term GHG emissions without relying on broader land-use change measures.

Materials and methods

The study quantified the effect of forwarding ruts on soil – atmosphere exchange of CO_2, CH_4, and N_2O in clearcuts on (i) moist organic soils (peat soils) and (ii) moist mineral soils. On organic soils, measurements were initiated in four clearcut objects harvested in winter 2022, with paired microsites established in a rut and in an adjacent undisturbed control area where machinery had not travelled; each paired design was replicated within each object (Table 1). The monitoring design provided post-harvest time series and, for part of the organic-soil objects, pre-harvest measurements derived from LIFE OrgBalt project monitoring program, enabling before – after context for interpretation of rut effects.

On moist mineral soils, the pilot component was implemented in two mature spruce stands harvested as clear-fellings in summer 2023. Measurement points were established in continuous deep ruts ($\geq$ 20 cm), and control points were located between strip-roads at 4-5 m distance from ruts; soil type was Podzolic Gley (Pzg).

In the organic-soil objects, each object contained two permanent plots (rut and control). Each plot included two collars (rings) for chamber gas sampling and three points for heterotrophic respiration measurements; each rut–control pair had one groundwater well for water-table monitoring.

In the moist mineral-soil pilot, the measurement programme included groundwater level, chamber-based sampling of CH_4 and N_2O for gas chromatography (with two permanent collars per location), field CO_2 measurements using an EGM5 analyser (three points per location), soil temperature at 10 cm depth, air temperature, and topsoil moisture. In water from groundwater wells, pH, electrical conductivity, redox potential, and dissolved O_2 were determined.

Table 1

Clearcut objects included in rut–control paired monitoring (A and B denote spatial replicates within each clearcut object)

Object ID	Forest stand ID	Soil	Plot	Latitude (X)	Longitude (Y)
LVMCA_R1	012-218 51	Organic	A	57.27927	25.85445
			B	57.27908	25.85455
LVMCA_R2	012-108 4	Organic	A	57.31107	25.93813
			B	57.31112	25.93724
LVMCA_R3	012-218 4	Organic	A	57.31116	25.93645
			B	57.31124	25.93574
LVMCA_R4	012-197 27	Organic	A	57.26859	25.9929
			B	57.26901	25.99285
LVMCA_R5	610-260 10	Mineral	B	56.72740	24.08985
LVMCA_R5	610-260 11	Mineral	A	56.72704	24.08938
LVMCA_R6	610-260 10	Mineral	B	56.72813	24.09089
LVMCA_R6	610-260 11	Mineral	A	56.72779	24.09095

The moist mineral-soil pilot plots were visited monthly during a 5-month campaign (24 July 2024 to 22 October 2024). Heterotrophic respiration was measured with a non-transparent chamber (0.023 m^3; diameter 31.5 cm; height 30.0 cm) over 180 s with three repetitions per location, flushing chambers before each measurement. For CH_4 and N_2O (and CO_2 in laboratory determination), opaque chambers were placed on permanent collars; 100 cm^3 gas samples were taken into glass bottles every 10 min over 30 min (four samples per series). The chamber volume for GC sampling was 0.0655 m^3 (bottom diameter 50 cm, top diameter 42.5 cm, height 39.5 cm). Because monitoring did not cover the full annual cycle, the study was designed to assess short-term post-harvest differences between ruts and controls rather than annual greenhouse gas budgets.

CH_4, N_2O and CO_2 concentrations in collected gas samples were analysed in the laboratory using a Shimadzu GC-2014 gas chromatograph (Shimadzu Corporation, Kyoto, Japan) equipped with an electron capture detector (ECD) for N_2O and a flame ionisation detector (FID) for CH_4 and CO_2 and a Loftfield autosampler. Gas sampling and analysis followed the manual closed-chamber approach described in [7] and the gas chromatographic approach described by [8]. Prior to analysis, the gas chromatograph was calibrated using certified standard gas mixtures spanning the expected concentration range of the samples, and calibration stability was checked by repeated analysis of control standards during the analytical run. Fluxes from concentration time series were calculated using the ideal gas law and the linear rate of concentration change in the chamber. Fluxes from GC time series were computed with a spreadsheet implementation of the ideal gas law–based conversion using chamber geometry and the linear rate of concentration change (δv). Measurements with insufficient linearity in CO_2 concentration change ($R^2 < 0.95$) were excluded. Heterotrophic respiration calculations used the R package *gasfluxes*, with automated trimming of the initial period (typically 30 s) to maximise the correlation coefficient. Gas flux from chamber GC series is calculated using Equation **Error! Reference source not found.**.

$$F_g = \frac{M \cdot P \cdot V \cdot \delta v}{R \cdot T \cdot A \cdot ppm} \text{ [µg C(N)·m}^{-2}\text{·h}^{-1}\text{]}, \quad (1)$$

where M – molar mass (CO_2 44.01 g mol^{-1}; CH_4 16.04 g mol^{-1}; N_2O 44.01 g mol^{-1});
P – atmospheric pressure, 101300 Pa;
V – chamber volume (0.0655 m^3 for GC chamber; 0.023 m^3 for respiration chamber);
R – universal gas constant, 8.3143 $m^3 \cdot Pa \cdot K^{-1} \cdot mol^{-1}$;
T – air temperature, K;
A – chamber footprint area (0.19625 m^2 and 0.076 m^2 for the respective chambers);
δv –concentration change rate in ppm (v) over time.

To compare the combined climatic effect of CO_2, CH_4 and N_2O, fluxes were expressed as CO_2 equivalents using 100-year global warming potentials of 28 for CH_4 and 265 for N_2O (Equation **Error! Reference source not found.**).

$$F_{CO2eq} = F_{CO_2} + 28 \cdot F_{CH_4} + 265 \cdot F_{N_2O}. \quad (2)$$

The experimental design consisted of paired rut-control comparisons in two soil groups. On organic soils, four independent clearcut objects were studied, each containing one rut plot and one adjacent control plot; each plot contained two permanent chamber collars, which were treated as within-plot subsamples and averaged by plot and sampling date prior to treatment-level comparison. On mineral soils, two clearcuts were studied, with two spatial replicates (plots A and B) per treatment in each clearcut; repeated monthly measurements yielded $n = 16$ observations per treatment across sampling rounds in the pilot dataset. Because the same plots were revisited over time, repeated measurements were not interpreted as independent spatial replicates.

Prior to inferential analysis, data distribution and homogeneity of variance were evaluated using the Shapiro-Wilk test together with visual inspection of histograms and normal probability plots. When parametric assumptions were met, differences between rut and control areas were tested using Welch's two-sample t-test; otherwise, the Wilcoxon rank-sum test was used. Because replication at the organic-soil object level was limited ($n = 4$ rut–control pairs), those results are presented primarily as means ± standard error and percentage differences, without further stratification. Relationships between GHG fluxes and environmental variables were analysed using correlation and regression analysis; Spearman's rank correlation was applied when normality assumptions were not met. Statistical significance was accepted at $p < 0.05$.

To support upscaling, rut extent was characterised using unmanned aerial vehicle-based light detection and ranging (UAV-LiDAR) and GIS processing. High-density UAV-LiDAR was acquired using a Zenmuse L1 sensor mounted on a DJI Matrice 300 platform, generating point clouds with ≥ 160 points per m^2. Point-cloud preprocessing and DEM generation were conducted in Global Mapper and CloudCompare, producing a 10 cm horizontal-resolution DEM for analysis.

Automatic rut detection was implemented by adapting an algorithm previously developed for automated drainage-ditch delineation from digital elevation models (DEMs) [9]. In its original application to 0.5-1.0 m DEMs, total ditch-network length was mapped with up to 96% accuracy in agricultural land and 90-95% in forests, depending on ditch type. The minimum detectable depression depth was 0.3 m (typical of seasonal ditches), while in some cases depressions as shallow as 0.2 m were detectable. These results support the assumption that much higher point-density UAV LiDAR (DJI Zenmuse L1; 150-200 points m^{-2} vs 4 points m^{-2} in national datasets) enables identification of smaller-scale terrain features consistent with forwarding ruts.

The algorithm was integrated into a QGIS tool and relies on logical raster queries in a moving-window framework to detect local depressions of a specified minimum depth (B, m) within a predefined maximum width (C, raster cells). A DEM cell (A) is classified as "rut" when neighbouring cells at distance ± C in multiple directions (orthogonal and diagonal) are higher than A by at least B, yielding a binary output (1/0) (Equation **Error! Reference source not found.**).

```
if(( A + B < A [-C,0] && + B < A [C,0])
|| (A + B < DEM [0,C] && A + B < DEM [0,-C])
|| (A + B < A [C,C] && A + B < A [-C,-C])
|| (A + B < A [-C,C] && A + B < A [C,-C]) ,1 ,0).   (3)
```

At regional scale (Kurzeme), stands were selected using national forest register data to ensure clearcuts in peatland forest types harvested shortly before LiDAR acquisition in two scanning cycles (2016 and 2022). Reference data were produced by manual rut mapping from DEM hillshade. Ruts were classified by width and depth using virtual cross-profiles at 2 m spacing (SAGA GIS Cross Profiles in QGIS). Relative to manual mapping, automated mapping produced 37% lower total rut length in first-cycle data.

Results and discussion

Paired rut–control comparisons showed a consistent shift in GHG exchange towards lower CO_2 efflux and substantially higher CH_4 emissions in ruts, while N_2O tended to decrease or remain statistically unchanged depending on soil group. In moist mineral soils, mean CO_2 fluxes in ruts were 144 $mg \cdot m^{-2} \cdot h^{-1}$ compared with 339 $mg \cdot m^{-2} \cdot h^{-1}$ in controls (-58%). Mean CH_4 fluxes shifted from a small net uptake in controls (-44 $\mu g \cdot m^{-2} \cdot h^{-1}$) to a strong net emission in ruts (1682 $\mu g \cdot m^{-2} \cdot h^{-1}$), while N_2O decreased from 29 to -10 $\mu g \cdot m^{-2} \cdot h^{-1}$ (-134%).

In organic soils, rut formation was associated with a smaller relative reduction in CO_2 (309 vs 362 $mg \cdot m^{-2} \cdot h^{-1}$; -15%) but a markedly stronger absolute and relative increase in CH_4 (7961 vs 1051 $\mu g \cdot m^{-2} \cdot h^{-1}$; + 657%). N_2O decreased from 41 to 19 $\mu g \cdot m^{-2} \cdot h^{-1}$ (-53%).

The mineral-soil pilot dataset comprised two Podzolic Gley clearcuts, two spatial replicates per treatment in each clearcut, and repeated monthly observations ($n = 16$ per treatment across sampling rounds). Mean CH_4-C was 495.78 $\mu g \cdot m^{-2} \cdot h^{-1}$ in ruts versus 4.25 $\mu g \cdot m^{-2} \cdot h^{-1}$ in controls, and the rut effect on CH_4 was significant ($t = -3.53$, $p = 0.002$). In contrast, N_2O-N and CO_2-C showed no significant rut–control differences ($p = 0.231$ and $p = 0.551$, respectively).

Environmental covariates in the mineral-soil pilot indicated generally moist and chemically weakly acidic conditions (mean soil moisture 42%, pH 5.42; groundwater level mean 148 cm). CO_2 efflux correlated negatively with soil moisture ($r = -0.56$, $p < 0.001$) and air temperature ($r = -0.49$, $p = 0.004$), whereas CH_4 fluxes showed no meaningful correlations with soil moisture or soil temperature, suggesting dominance of local anaerobic microsites rather than plot-scale gradients. Mean results are provided in Fig. 1.

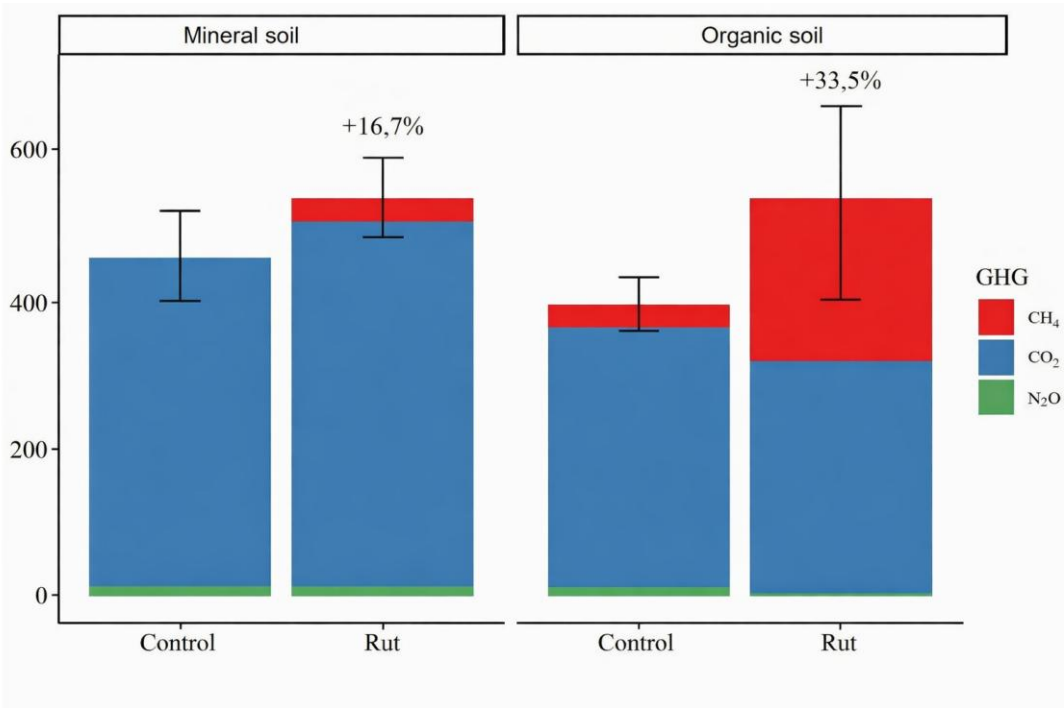

Fig. 1. **Mean GHG fluxes in ruts and controls**

Across both soil groups, rut formation shifted the system towards stronger methane emission and weaker carbon dioxide efflux, consistent with a physical mechanism in which compaction reduces gas diffusivity and increases water-filled pore space. The rut-driven CH_4 response differed strongly by soil type: organic soils exhibited substantially higher absolute CH_4 fluxes in ruts than moist mineral soils (7961 vs 1682 $\mu g \cdot m^{-2} \cdot h^{-1}$), consistent with higher availability of labile carbon and a greater propensity for persistent anoxia in peat substrates. In moist mineral soils, rutting was sufficient to flip CH_4 exchange from net uptake to net emission, indicating that even where groundwater levels are relatively deep, compaction can generate anaerobic hotspots in the upper soil layers that dominate methane dynamics.

Our results show that rut formation altered greenhouse gas exchange primarily through methane. Total GHG emissions expressed as CO_2 equivalents were 16.7% higher in ruts on moist mineral soils and 33.5% higher in ruts on organic soils than in adjacent undisturbed control microsites. This pattern

indicates a clear soil-type dependence of the rut effect and suggests that rutting acts as a microtopographic disturbance creating wetter and less aerated microsites, particularly in organic soils where high water-holding capacity and abundant organic substrate favour anaerobic conditions.

The CO_2 reductions in ruts (-58% in moist mineral soils; -15% in organic soils) are consistent with oxygen limitation constraining aerobic decomposition and root/microbial respiration, although the relative magnitude differed. A plausible interpretation is that in moist mineral soils, baseline aerobic respiration between strip-roads remains comparatively high and is more strongly suppressed when diffusion pathways are disrupted, whereas in organic soils the background respiration signal is already moisture constrained and therefore shows a smaller proportional decline. The mineral-soil pilot further indicates that CO_2 efflux is sensitive to moisture and air temperature variability, which implies that rut–control contrasts in CO_2 may be seasonally unstable and require multi-season sampling to characterise with low uncertainty.

For N_2O, both soil groups exhibited lower mean fluxes in ruts in the aggregated dataset, and the mineral-soil pilot detected no significant rut effect despite higher mean N_2O in controls. This pattern is consistent with the expectation that strongly reduced conditions can either enhance complete denitrification to N_2 (thereby decreasing N_2O) or, under fluctuating redox, produce pulses that are not captured by monthly sampling. Therefore, the absence of a consistent rut signal for N_2O does not imply irrelevance; rather, it implies that temporal dynamics (episodic events after rainfall, freeze–thaw, or residue decomposition) likely govern net differences, and that sampling frequency and event-based campaigns may be necessary to resolve the N_2O component robustly.

The lower CO_2 fluxes in ruts can be interpreted as a consequence of reduced aerobic decomposition under oxygen-limited conditions. This agrees with studies showing that CO_2 emissions from organic soils are jointly controlled by temperature and aeration, and that hydrological disturbance can locally suppress aerobic mineralisation despite continued substrate availability [10; 11]. In contrast, the N_2O response was weak and inconsistent, which is also plausible from a process perspective. N_2O production depends on transient interactions among mineral N availability, soil moisture, and denitrification completeness; under strongly reduced conditions, N_2O may be further reduced to N_2. Similar studies on organic soils have reported comparatively low or highly variable N_2O fluxes and weak relationships with single environmental variables [12; 13].

From a climate-accounting perspective, the principal implication is that rut formation can significantly increase the warming-relevant component of GHG exchange even when CO_2 efflux decreases, because methane's radiative efficiency makes relatively small CH_4 mass flux changes climatically influential. This is especially evident in organic soils where rut CH_4 emissions are an order of magnitude higher than controls, suggesting that rut area and persistence may become critical determinants of post-harvest GHG balance. In moist mineral soils, the "sign reversal" from CH_4 uptake to emission indicates that rut occurrence may convert sites traditionally treated as weak CH_4 sinks into episodic sources, which could be relevant for stand-level assessments if rut extent is non-trivial.

The stronger CH_4 response in ruts on organic soils is consistent with peatland studies showing that shallower water tables and restricted oxygen diffusion shift the balance from CH_4 oxidation towards methanogenesis. In peat soils, wetter conditions generally enhance CH_4 production, whereas more aerated conditions suppress methanogenesis and may allow net CH_4 uptake. Similar hydrological controls have been reported for peatlands and managed organic soils, where groundwater level and oxygen availability were identified as primary controls of CH_4 emissions [11; 14]. Our results extend this mechanism to forwarding ruts in forest clearcuts, suggesting that rut depressions can function as localized anaerobic hotspots even when surrounding areas remain less saturated.

A key remaining uncertainty for both soil groups is the duration of rut effects. The dataset demonstrates clear short-term functional shifts, but translating these into annualised impacts requires resolving how quickly ruts drain, infill, revegetate, and recover aeration, as well as how rut severity modulates methane production. The observed lack of correlation between CH_4 and plot-scale moisture/temperature in the mineral-soil pilot supports the hypothesis that rut morphology and microsite conditions (local ponding, residue-soil mixing, and compaction gradients) may be stronger predictors than stand-average environmental variables, motivating a combined approach that couples flux measurements with rut severity metrics for upscaling.

Automatic identification of wheel ruts using LiDAR data was carried out in 12 forest stands. The results indicate that the use of airborne laser scanning data together with the methodology developed in this study identified a substantially greater total rut length compared to field measurements. Among the analyzed areas, the highest total rut length per hectare was observed in forest stand 610-261-11, where rut length reached 459 m ha^{-1} (625 m in total). Field measurements in this stand recorded 227 m of ruts; however, LiDAR measurements count a 1-m segment with two parallel ruts as 2 m of total rut length. This approach is appropriate for characterising rut total area and its impact on greenhouse gas emissions, as it ensures a conservative approach and does not artificially reduce the potential effect on GHG emissions.

The novelty of this study lies in the paired rut–control comparison across both organic and moist mineral forest soils after clearfelling, focusing on a disturbance type that is operationally important but usually omitted from stand-level GHG assessments. A further novel aspect is the linkage of chamber-based flux measurements with rut detection and mapping, which provides a basis for future upscaling. The main limitations are the limited number of study objects, relatively high between-object variability, the short monitoring period, and the currently unknown persistence of elevated emissions from ruts, especially CH_4. Therefore, the reported values should be interpreted as short-term plot-scale estimates rather than annual stand-level emission factors.

The results should be interpreted in the context of the relatively short monitoring period, which captured only a limited part of the annual cycle and therefore cannot fully represent seasonal variability of greenhouse gas fluxes. This is particularly important for CH_4 and N_2O, which are often episodic and can respond strongly to short-term changes in soil moisture, water-table position, temperature, and rainfall events. Consequently, the observed rut effect should be regarded as a short-term post-harvest signal rather than an annual emission factor. Additional measurements covering spring rewetting, summer drying, autumn transition, and winter or freeze–thaw conditions would be necessary to determine whether the differences between ruts and controls persist, weaken, or intensify across seasons.

Conclusions

1. The obtained measurements provide an empirical basis to quantify short-term rut effects on CO_2, CH_4 and N_2O fluxes using paired rut – control microsites.
2. Rut formation consistently shifted GHG exchange relative to intact soil. CO_2 fluxes were lower in ruts (≈50% lower on moist mineral soils; ≈15% lower on organic soils), N_2O was also lower (reported mean decreases of 134% on mineral soils and 53% on organic soils), whereas CH_4 increased sharply, indicating oxygen limitation under higher moisture as a dominant control of rut-driven responses; rut depth–moisture–bulk density linkages should be tested as predictors, and CO_2 comparisons may require correction for vegetation differences at measurement points.
3. Upscaling is constrained primarily by missing activity data. Stand- and regional-scale impacts cannot be robustly derived without quantifying rut extent and severity under production conditions (both thinning and regeneration felling), particularly where harvesting occurs under wet conditions.
4. National-scale rut mapping is feasible from LiDAR-derived DEMs, but reliable detection requires high spatial resolution (0.2 m), which increases data volume and processing time; performance is sensitive to point density and acquisition conditions (seasonality, canopy, surface wetness), and rut detection may fail in vegetation-season datasets or exceptionally wet areas during scanning.
5. Harvester/forwarder GPS tracks are a key enabling dataset for separating recent ruts from morphologically similar linear features (e.g., ditches) and for constraining detection to the latest operation; without tracks, additional spatial filters (e.g., compartment boundaries) are required to reduce misclassification.
6. Automated rut mapping is expected to underestimate total rut length relative to manual interpretation (reported difference ~37%); repeated LiDAR cycles can quantify temporal changes in rut length and support assessment of rut persistence and the influence of stand regeneration on rut visibility.

Acknowledgements

The study is elaborated within the scope of the research program "Carbon turnover in forest ecosystem" grant No. 5_5.9.1_0081_101_21_87. Contribution of Andis Lazdiņš was funded by the project 6.1.1.2/1/25/A/001 "Research and Innovation Based Solutions to Support the Peat Sector's Transition to a Climate Neutral Economy (PeatTransform)". Contribution of Raitis Normunds Meļņiks was funded by the project lzp-2024/1-0484 "Comprehensive analysis of hemiboreal forest structure, species composition and ecosystem services using VHR hyperspectral and LiDAR data".

Author contributions:

Conceptualization, A.L. and R.N.M.; methodology, A.L. and R.N.M.; validation, A.B.; formal analysis, A.B. and R.N.M.; data curation, A.B. and M.V.D.; writing – original draft preparation, A.L. and Z.A.Z.; writing – review and editing, R.N.M. and A.B.; visualization, A.B.; project administration, A.L.; funding acquisition, A.L. All authors have read and agreed to the published version of the manuscript.

References

[1] Teepe R., Brumme R., Beese F., Ludwig B. Nitrous Oxide Emission and Methane Consumption Following Compaction of Forest Soils, Soil Science Soc of Amer J, vol. 68, no. 2, 2004, pp. 605-611, DOI: 10.2136/sssaj2004.6050

[2] Uusitalo J., Ala-Ilomäki J., Lindeman H., Toivio J., Siren M. Predicting rut depth induced by an 8-wheeled forwarder in fine-grained boreal forest soils, Annals of Forest Science, vol. 77, no. 2, 2020, Art. no. 2, DOI: 10.1007/s13595-020-00948-y

[3] Mohtashami S., Eliasson L., Jansson G., Sonesson J. Influence of soil type, cartographic depth-to-water, road reinforcement and traffic intensity on rut formation in logging operations: a survey study in Sweden, Silva Fenn., vol. 51, no. 5, 2017, DOI: 10.14214/sf.2018

[4] Nazari M. et al. Impacts of Logging-Associated Compaction on Forest Soils: A Meta-Analysis, Front. For. Glob. Change, vol. 4, 2021, p. 780074, DOI: 10.3389/ffgc.2021.780074

[5] Crawford L. J., Heinse R., Kimsey M. J., Page-Dumroese D. S. Soil Sustainability and Harvest Operations: a Review, U.S. Department of Agriculture, Forest Service, Rocky Mountain Research Station, Fort Collins, CO, RMRS-GTR-421, 2021. DOI: 10.2737/RMRS-GTR-421

[6] Lazdins A., Butlers A., Purvina D. Results of pilot study comparing greenhouse gas fluxes from forwarding ruts and control area in moist mineral soil after clearfelling, presented at the 24th International Scientific Conference Engineering for Rural Development, May 2025. DOI: 10.22616/ERDev.2025.24.TF015

[7] Hutchinson G. L., Livingston G. P. Use of chamber systems to measure trace gas fluxes, ASA special publication (USA), 1993, Accessed: Dec. 27, 2017. [Online]. Available: http://agris.fao.org/agris-search/search.do?recordID = US9423815

[8] Loftfield N., Flessa H., Augustin J., Beese F. Automated Gas Chromatographic System for Rapid Analysis of the Atmospheric Trace Gases Methane, Carbon Dioxide, and Nitrous Oxide, Journal of Environment Quality, vol. 26, no. 2, 1997, p. 560, DOI: 10.2134/jeq1997.00472425002600020030x

[9] Melniks R., Ivanovs J., Lazdins A., Makovskis K. Mapping drainage ditches in agricultural landscapes using LiDAR data, Agronomy research, vol. 20, no. 2, 2022, pp. 318-325, DOI: 10.15159/AR.22.012

[10] Clark L., Strachan I. B., Strack M., Roulet N. T., Knorr K.-H., Teickner H. Duration of extraction determines CO2 and CH4 emissions from an actively extracted peatland in eastern Quebec, Canada, Biogeosciences, vol. 20, no. 3, 2023, pp. 737-751, DOI: 10.5194/bg-20-737-2023

[11] Oestmann J., Dettmann U., Düvel D., Tiemeyer B. Experimental warming increased greenhouse gas emissions of a near-natural peatland and Sphagnum farming sites, Plant Soil, vol. 480, no. 1, 2022, pp. 85-104, DOI: 10.1007/s11104-022-05561-8

[12] Hatano R. Impacts of changes in peat soils due to agricultural activities on greenhouse gas (especially N2O) emissions and their mitigations, Pedosphere, vol. 35, no. 1, 2025, pp. 8-11, DOI: 10.1016/j.pedsph.2023.12.010

[13] Yao Z. et al. Soil C/N ratio is the dominant control of annual N2O fluxes from organic soils of natural and semi-natural ecosystems, Agricultural and Forest Meteorology, vol. 327, 2022, p. 109198, DOI: 10.1016/j.agrformet.2022.109198
[14] Huang Y. et al. Tradeoff of CO2 and CH4 emissions from global peatlands under water-table drawdown, Nat. Clim. Chang., vol. 11, no. 7, 2021, pp. 618-622, DOI: 10.1038/s41558-021-01059-w